molecular pharmaceutics

articles

N-Hydroxy-7-(2-naphthylthio) Heptanomide Inhibits Retinal and Choroidal Angiogenesis

Jeong Hun Kim,[†,‡] Jin Hyoung Kim,[†,‡] Meeyeon Oh,[‡,§] Young Suk Yu,[†] Kyu-Won Kim,[||] and Ho Jeong Kwon*[,§]

Chemical Genomics Laboratory, Department of Biotechnology, College of Life Science & Biotechnology, Yonsei University, Seoul 120-749, Korea, Department of Ophthalmology, College of Medicine, Seoul National University & Seoul Artificial Eye Center Clinical Research Institute, Seoul National University Hospital, Seoul 110-744, Korea, and NeuroVascular Coordination Research Center, College of Pharmacy and Research Institute of Pharmaceutical Sciences, Seoul National University, Seoul 151-742, Korea

Received September 24, 2008; Revised Manuscript Received November 26, 2008; Accepted January 2, 2009

Abstract: Histone deacetylase (HDAC) is a key enzyme regulating gene expression, including angiogenic cytokine expression. We have previously identified a novel synthetic HDAC inhibitor, known as *N*-hydroxy-7-(2-naphthylthio) heptanomide (HNHA), with antitumor properties. Here, we investigated the antiangiogenic properties of this small synthetic molecule both *in vitro* and *in vivo*. HNHA inhibited nuclear HDAC enzyme activity in human umbilical endothelial cells (HUVECs), an effect accompanied by histone hyperacetylation, p21 upregulation, and cell cycle arrest. HNHA also inhibited vascular endothelial growth factor-induced tube formation and migration of HUVECs, in the absence of any detectable cellular toxicity. Intravitreous injection of HNHA into mice inhibited retinal neovascularization associated with oxygen-induced retinopathy (OIR) and laser-induced choroidal neovascularization (CNV), as determined through fluorescence angiography and vessel counting. Retinas from HNHA-treated animals had a normal histological appearance without any detectable increase in terminal deoxynucleotidyl transferase-mediated dUTP nick-end labeling-positive cells, showing that this compound did not induce retinal toxicity. These findings indicate that HNHA has direct antiangiogenic effects and may be an effective strategy for inhibiting the pathological retinal and choroidal neovascularization underlying blinding eye diseases.

Keywords: Anti-angiogenesis; choroidal neovascularization; histone deacetylase inhibitor; *N*-hydroxy-7-(2-naphthylthio) heptanomide; retinal neovascularization

Introduction

The formation of new blood vessels from preexisting capillaries, or angiogenesis, is tightly controlled by a balance of positive and negative regulatory factors.[1] This process normally only occurs during development and tissue repair; however, pathological forms of angiogenesis exist, particularly within the eye. This is the most common cause of blindness at all ages and underlies conditions such as retinopathy of prematurity (ROP) in children, diabetic retinopathy in young adults, and age-related macular degeneration (AMD) in the elderly.[2] Angiogenic factors, such as vascular endothelial growth factor (VEGF) and fibroblast growth factor, induce the production and secretion of matrix metalloproteases and plasminogen activators by endothelial cells, enabling these cells to digest the basement membrane and invade the surrounding tissue.[3] VEGF, in particular, is a potent angiogenic and vascular permeability-enhancing

* To whom correspondence should be addressed. Chemical Genomics Laboratory, Department of Biotechnology, College of Life Science & Biotechnology, Yonsei University, Seoul 120-749, Republic of Korea. Tel: 82-2-2123-5883. Fax: 82-2-362-7265. E-mail: kwonhj@yonsei.ac.kr.

[†] Seoul National University Hospital.

[‡] These authors contributed equally to this work.

[§] Yonsei University.

[||] Seoul National University.

(1) Folkman, J. Angiogenesis. *Annu. Rev. Med.* **2006**, *57*, 1–18.

(2) Aiello, L. P. Vascular endothelial growth factor in ocular fluid of patients with diabetic retinopathy and other retinal disorders. *N. Engl. J. Med.* **1994**, *331*, 1480–1487.

10.1021/mp800178b CCC: $40.75
Published on Web 02/03/2009

factor triggering retinal neovascularization associated with ROP and choroidal neovascularization (CNV) associated with AMD.[4]

In ROP, retinal neovascularization is followed by the vessel loss, leading to retinal hypoxia. During retinal neovascularization, fragile and leaky vessels are formed at the junction between the vascular and avascular zone of the retina. Over time, these proliferative vessels induce a fibrous scar extending from the retina to the vitreous gel, resulting a retinal detachment and, likely, blindness.[5] Therefore, strategies for treating pathological angiogenesis associated with ROP include either blocking the vessel loss to prevent hypoxia or directly inhibiting vessel proliferation.[6] Oxygen-induced retinopathy (OIR) is the most widely used mouse model of retinal neovascularization. In this model, newborn mice undergo hyperoxia-induced vaso-obliteration of capillaries and are then returned to normoxic conditions.[7] This triggers pathological angiogenesis in the inner retina, causing newly formed capillaries to break through the internal limiting membrane and spread into the vitreous.[8]

CNV leads to severe vision loss in AMD patients, although the exact underlying mechanism has yet to be identified.[9] CNV is a biphasic process that is initiated with rupture of Bruch's membrane and is followed by proliferation of the choroidal vessels, which invade the subretinal space. The most common model of CNV is laser photocoagulation-induced rupture of Bruch's membrane, which stimulates proliferation of vascular endothelial cells in pre-existing choroidal capillary networks.[10]

Histone acetylation regulates gene transcription in many cell types.[11] Histone deacetylase (HDAC) is known to participate in the silencing of a number of genes.[12,13] We have previously shown that this protein also participates in hypoxia-induced angiogenesis.[14] Specific HDAC inhibitors have been used to elucidate HDAC function and have been proposed as a therapy for some types of cancer. The synthetic HDAC inhibitor, suberoylanilide hydroxamic acid (SAHA),[15] was recently launched as the first clinical antitumor drug of this class of inhibitors.[16] We recently discovered a small synthetic HDAC inhibitor, *N*-hydroxy-7-(2-naphthylthio) heptanomide (HNHA), which has *in vitro* and *in vivo* antitumor activity comparable to SAHA.[17] Here, we investigated the antiangiogenic properties of HNHA in human umbilical vein endothelial cells (HUVECs) and in mice with the OIR or laser photocoagulation-induced CNV.

Table 1. HDAC-Inhibiting and Antiproliferative Activity of HNHA and SAHA

	IC_{50} (μM)	
inhibitor	HDAC inhibition	inhibition of HUVEC proliferation
SAHA	0.05 ± 0.005	2 ± 0.41
HNHA	0.1 ± 0.01	7.5 ± 0.82

Results

HNHA Inhibits *in Vitro* HDAC activity and proliferation of HUVECs. HNHA has previously been shown to have antitumor activity in human fibrosarcoma cells (HT1080).[17] We analyzed the effect of HNHA on histone deacetylase inhibition and cellular proliferation in HUVECs. *In vitro* HDAC assays revealed that HNHA exhibited potent HDAC-inhibitory activity with an IC_{50} value of 0.1 μM (Table 1). The HDAC-inhibiting activity of HNHA was slightly less potent than that of SAHA, which had an IC_{50} of 0.05 μM. The addition of either HDAC inhibitor gradually reduced cellular growth in a time- and dose-dependent manner, with an IC_{50} value of 7.5 μM for HNHA and 2.0 μM for SAHA (Table 1). The antiproliferative effects of HNHA were accompanied by the appearance of a more elongated cellular shape (data not shown), a morphological change similar to that seen in SAHA-treated cells.

HNHA Induces Histone Hyperacetylation, Increases $p21^{WAF1}$ Expression, and Inhibits Cell Cycle Progression in HUVECs. Inhibition of HDAC activity by specific inhibitors induces histone hyperacetylation. HDAC6 also regulates tubulin acetylation status, leading to changes in the

(3) Risau, W. Mechanisms of angiogenesis. *Nature* **1997**, *386*, 671–674.
(4) Adamis, A. P.; Shima, D. T. The role of vascular endothelial growth factor in ocular health and disease. *Retina* **2005**, *25*, 111–118.
(5) Roth, A. M. Retinal vascular development in premature infants. *Am. J. Ophthalmol.* **1977**, *84*, 636–640.
(6) Chen, J.; Smith, L. E. Retinopathy of prematurity. *Angiogenesis* **2007**, *10*, 133–140.
(7) Smith, L. E. Oxygen-induced retinopathy in the mouse. *Invest. Ophthalmol. Vis. Sci.* **1994**, *35*, 101–111.
(8) Pierce, E. A.; Foley, E. D.; Smith, L. E. Regulation of vascular endothelial growth factor by oxygen in a model of retinopathy of prematurity. *Arch. Ophthalmol.* **1996**, *114*, 1219–1228.
(9) Macular Photocoagulation Group. Argon laser photocoagulation for neovascular maculopathy. Five-year results from randomized clinical trials. Macular Photocoagulation Study Group. *Arch. Ophthalmol.* **1991**, *109*, 1109−1114.
(10) Miller, H.; Miller, B.; Ryan, S. J. The role of retinal pigment epithelium in the involution of subretinal neovascularization. *Invest. Ophthalmol. Vis. Sci.* **1986**, *27*, 1644–1652.
(11) Grunstein, M. Histone acetylation in chromatin structure and transcription. *Nature* **1997**, *389*, 349–352.
(12) Taunton, J.; Hassig, C. A.; Schreiber, S. L. A mammalian histone deacetylase related to the yeast transcriptional regulator Rpd3p. *Science* **1996**, *272*, 408–411.
(13) Hassig, C. A. Histone deacetylase activity is required for full transcriptional repression by mSin3A. *Cell* **1997**, *89*, 341–347.
(14) Kim, M. S. Histone deacetylases induce angiogenesis by negative regulation of tumor suppressor genes. *Nat. Med.* **2001**, *7*, 437–443.
(15) Richon, V. M. Second generation hybrid polar compounds are potent inducers of transformed cell differentiation. *Proc. Natl. Acad. Sci. U.S.A.* **1996**, *93*, 5705–5708.
(16) Mann, B. S. FDA approval summary: vorinostat for treatment of advanced primary cutaneous T-cell lymphoma. *Oncologist.* **2007**, *12*, 1247–1252.
(17) Kim, D. H. Anti-tumor activity of N-hydroxy-7-(2-naphthylthio) heptanomide, a novel histone deacetylase inhibitor. *Biochem. Biophys. Res. Commun.* **2007**, *356*, 233–238.

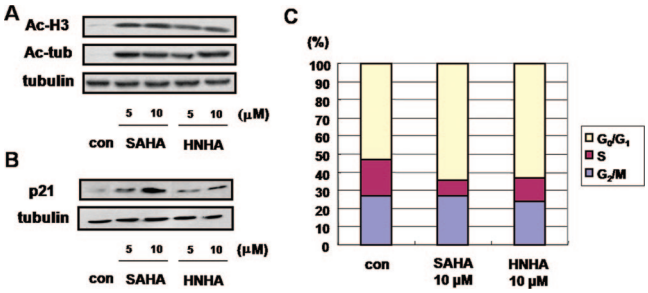

Figure 1. HNHA inhibits HDAC activity and cell growth. (A) Western blot analysis of acetylated histone (Ac-H3) and acetylated tubulin (Ac-tubulin) or (B) $p21^{WAF1}$ in HUVECs treated with SAHA or HNHA. Tubulin served as an internal control in B. (C) FACS analysis of DNA content following a 24 h treatment of HUVECs with HNHA or SAHA.

stability of dynamic microtubules.[18−20] Western blot analysis of hyperacetylated histones and tubulin in HUVECs revealed that highly acetylated forms of both proteins accumulated in response to HNHA treatment, but not DMSO (control) treatment (Figure 1A). We also investigated the effect of HNHA on the expression of $p21^{WAF1}$, a protein known to be induced by histone hyperacetylation and known to play a critical role in the HDAC inhibitor-induced cell cycle arrest.[21−23] Treatment of HUVECs with HNHA or SAHA for 12 h increased $p21^{WAF1}$ protein levels by 46% (Figure 1B). The ability of HNHA to relieve suppression of $p21^{WAF1}$ in HUVECs suggests that this compound may induce cell cycle arrest in these cells.[21,24] Indeed, flow cytometric analysis revealed that a 24 h treatment of synchronized HUVECs with HNHA increased the number of G_0/G_1 phase cells by 70% and reduced the number of S phase cells by 8% (Figure 1C). SAHA elicited a similar inhibition of cell cycle progression that was inhibited by HNHA.

HNHA Inhibits VEGF-Induced Angiogenesis in HUVECs. *In vitro* tube formation and cell invasion assays were conducted to assess the effect of 1−10 μM HNHA on the angiogenic phenotype of HUVECs. This concentration range was selected based on the finding that concentrations of HNHA up to 10 μM did not significantly affect HUVEC viability (Figure 2A). In *in vitro* tube formation assays, serum-starved HUVECs were cultured on growth factor-reduced Matrigel in the presence of the angiogeneic factor, VEGF. After 18 h in the presence of VEGF, cultures formed elongated and robust tubelike structures that incorporated a much larger number of cells than structures in non-VEGF-treated cultures. Importantly, inclusion of HNHA inhibited VEGF-induced tube formation in a dose-dependent manner (Figure 2B,D). HNHA had a similar inhibitory effect on VEGF-induced HUVEC invasion, as assessed using Transwell migration chambers. As shown in Figures 2C and 2E, the 16 h incubation with VEGF increased the number of invaded cells by 100%, while HNHA reduced VEGF-induced invasion by 50%.

HNHA Inhibits Oxygen-Induced Retinal Neovascularization. Next, we determined whether HNHA could reduce retinal neovascularization in mice with OIR. OIR was induced by exposing mice at postnatal day 7 (P7) to 75% hyperoxia for 5 days. HNHA or SAHA (10 μM/1 μL) was intravitreously injected on P14, since neovascularization begins upon return to normoxia and peaks at P17.[25,26] Retinas from P17 control mice contained many neovascular tufts of intravitreous neovascularization at the junction between the vascularized and nonvascularized retina (Figure 3A). In contrast, retinas from P17 SAHA- (Figure 3B) or HNHA-treated (Figure 3C) mice showed markedly reduced retinal neovascularization. To measure intravitreous neovascularization in these animals, we counted vascular lumens between posterior surface of lens and anterior surface of the inner limiting membrane. The number of neovascular lumens was greater in retinas from P17 control mice (19 ± 3.6, Figure 3D) than in retinas from P17 SAHA- (4 ± 2.5, Figure 3E) or HNHA- (3 ± 1.7, Figure 3F) treated mice ($P < 0.05$ for either treatment vs control, Figure 3G).

HNHA Inhibits Laser Photocoagulation-Induced CNV. The effect of HNHA on laser-photocoagulation-induced CNV was also investigated. In these experiments, SAHA or HNHA (10 μM/1 μL) was intravitreously injected 10 days after laser photocoagulation based on previous data showing that active neovascularization begins at this time.[27] Angiographs clearly showed CNV with diffuse leakage at the laser photocoagulation site in control animals (Figure 4A). Both effects were much less evident in retinas from SAHA- (Figure 4B) or HNHA-treated animals (Figure 4C). Quantification of CNV by counting vessels in the subretinal fibrovascular membrane revealed that the number of neovascular lumens in retinas from control mice (14 ± 2.9, Figure 4D) exceeded that in retinas from SAHA- (5 ± 2.2, Figure 4E) or HNHA- (4 ±

(18) Haggarty, S. J. Domain-selective small-molecule inhibitor of histone deacetylase 6 (HDAC6)-mediated tubulin deacetylation. *Proc. Natl. Acad. Sci. U.S.A.* **2003**, *100*, 4389–4394.
(19) Zhang, Y. HDAC-6 interacts with and deacetylates tubulin and microtubules in vivo. *EMBO J.* **2003**, *22*, 1168–1179.
(20) Matsuyama, A. In vivo destabilization of dynamic microtubules by HDAC6-mediated deacetylation. *EMBO J.* **2002**, *21*, 6820–6831.
(21) Han, J. W. Apicidin, a histone deacetylase inhibitor, inhibits proliferation of tumor cells via induction of p21WAF1/Cip1 and gelsolin. *Cancer. Res.* **2000**, *60*, 6068–6074.
(22) Archer, S. Y. p21(WAF1) is required for butyrate-mediated growth inhibition of human colon cancer cells. *Proc. Natl. Acad. Sci. U.S.A.* **1998**, *95*, 6791–6796.
(23) Park, J. K. Augmentation of sodium butyrate-induced apoptosis by phosphatidylinositol 3-kinase inhibition in the human cervical cancer cell-line. *Cancer Res. Treat.* **2006**, *38*, 112–117.
(24) Xiao, H.; Hasegawa, T.; Isobe, K. Both Sp1 and Sp3 are responsible for p21waf1 promoter activity induced by histone deacetylase inhibitor in NIH3T3 cells. *J. Cell. Biochem.* **1999**, *73*, 291–302.
(25) Kim, J. H. Homoisoflavanone inhibits retinal neovascularization through cell cycle arrest with decrease of cdc2 expression. *Biochem. Biophys. Res. Commun.* **2007**, *362*, 848–852.
(26) Kim, J. H.; et al. Deguelin inhibits retinal neovascularization by down-regulation of HIF-1alpha in oxygen-induced retinopathy. *J. Cell. Mol. Med.* **2008** [Epub ahead of print].

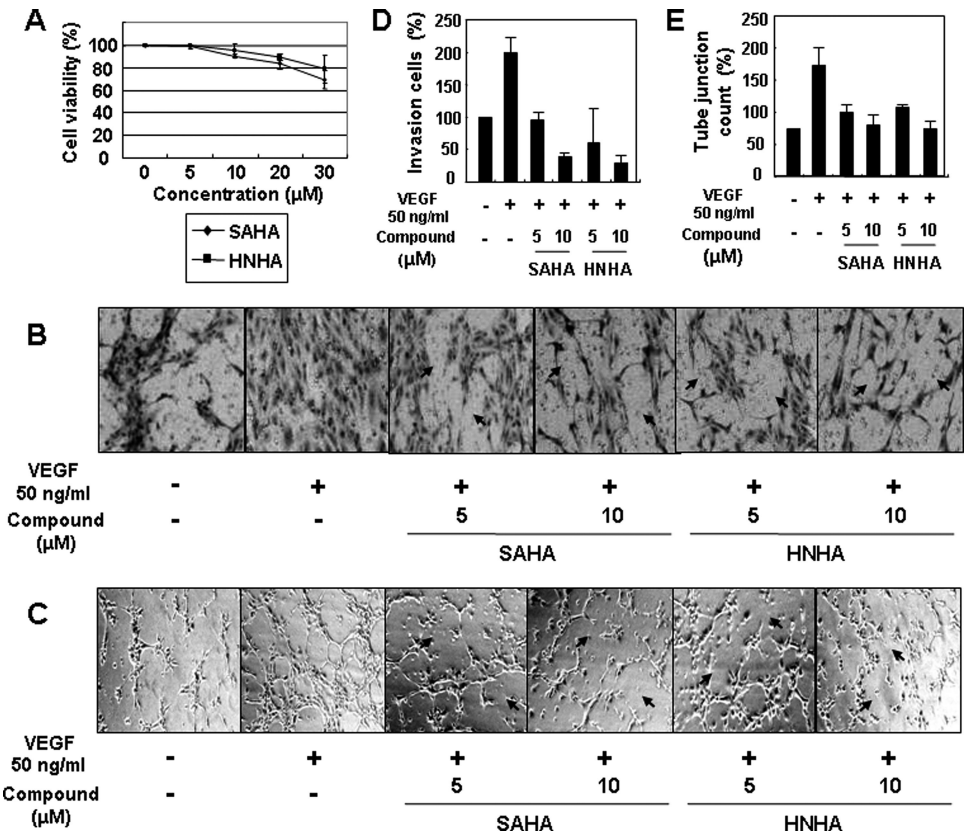

Figure 2. HNHA inhibits VEGF-induced angiogenesis in HUVECs. (A) Dose dependent effect of HNHA or SAHA on HUVEC viability after 3 days of treatment. Effect of HNHA or SAHA on VEGF-induced (B) tube formation and (C) migration in serum-starved HUVECs. The graphs show the inhibited angiogenesis, as quantified by measuring (D) invasive cells and (E) tube junctions. Quantitative analysis of cell invasion and tube formation from three independent experiments is shown.

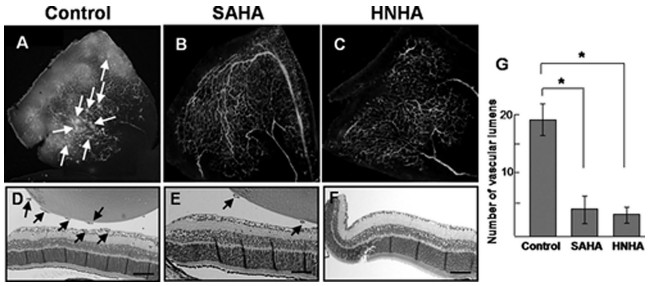

Figure 3. HNHA inhibits oxygen-induced retinal neovascularization. Fluorescein angiography showing whole-mounted retinas from P17 (A) control, (B) SAHA-treated, and (C) HNHA-treated mice with OIR. Arrows indicate intravitreous tufts of neovascularization. These experiments were repeated over three times with similar results. Hematoxylin-stained retinal cross sections prepared from P17 (D) control, (E) SAHA-treated, and (F) HNHA-treated mice with OIR. The lumens of new vessels growing into the vitreous are indicated with arrows. Scale bar, 200 μm in D−F. (G) Quantification of neovascular lumens. *P < 0.05 for control vs SAHA- or HNHA-treated mice ($n \geq 3$ for all groups).

1.1, Figure 4F) treated mice ($P < 0.05$ for either treatment vs control, Figure 4G).

Retinal Toxicity of HNHA. The retinal toxicity of 10 μM/1 μL SAHA or HNHA was evaluated through histological examination and terminal deoxynucleotidyl transferase-mediated dUTP nick-end labeling (TUNEL) of retinal tissue. As shown in Figure 5, retinas from SAHA- or HNHA-treated animals were of normal thickness, and all retinal layers were clear without any inflammatory cells in the vitreous, retina, or choroid. The number of TUNEL-positive cells in retinas from SAHA- or HNHA-treated animals was similar to that in control retinas (Figure 5).

Discussion

HNHA was first synthesized as a novel histone deacetylase inhibitor to have an antitumor activity in human fibrosarcoma cells (HT1080) by our group.[17] In the present study, HNHA increased the accumulation of highly acetylated histone and tubulin and gradually inhibited the HUVECs growth in a time- and dose-dependent manner. It is well-known that the expression of $p21^{WAF1}$, an inhibitor of cyclin/cyclin-dependent kinase complexes, was increased by the hyperacetylation of histones.[21−23] HNHA increased the accumulation of $p21^{WAF1}$ which was related to the inhibition of cell cycle progression: the increase of G_0/G_1 phase and the decrease of S phase (Figure 1). These biological activities of HNHA were similar to those of SAHA.

In addition, we demonstrated that HNHA, as a new HDAC inhibitor, has an antiangiogenic activity to retinal and

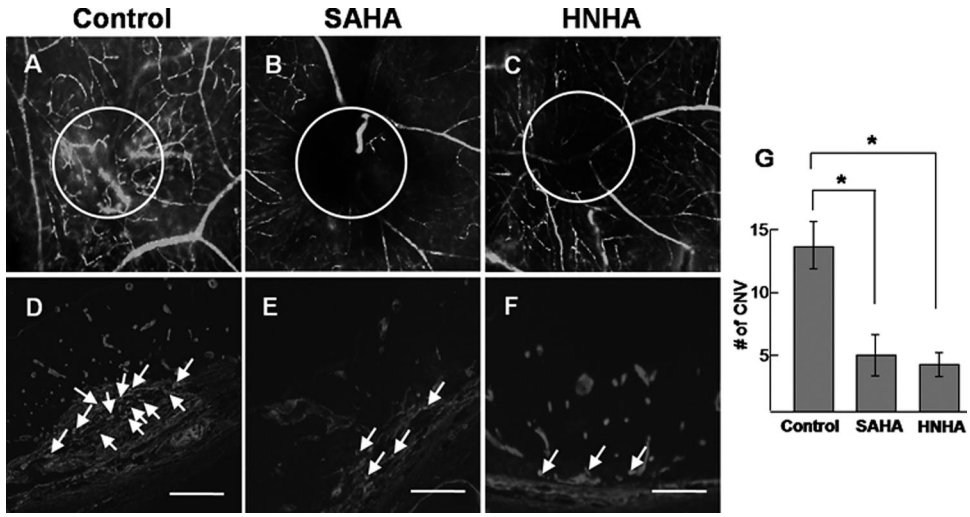

Figure 4. HNHA inhibits CNV induced by laser-photocoagulation. Fluorescein angiography showing whole-mounted retinas from (A) control, (B) SAHA-treated, and (C) HNHA-treated mice. Areas of CNV at the laser-photocoagulation site are circled. Hematoxylin-stained retinal cross sections prepared from (D) control, (E) SAHA-treated, and (F) HNHA-treated mice subjected to laser-photocoagulation. New vessels growing from choroidal vessels are indicated with arrows. Scale bar, 50 μm in D−F. (G) Quantification of neovascular lumens (*$P < 0.05$).

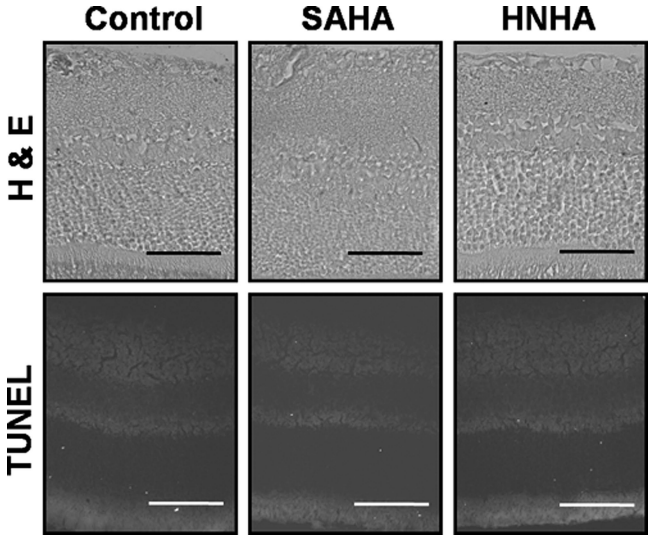

Figure 5. Retinal toxicity of HNHA. Hematoxylin and TUNEL staining of retinas from SAHA- or HNHA-treated animals. 0.10 μM SAHA or HNHA was intravitreously injected, and the globes were enucleated 3 days after treatment. No inflammatory cells could be detected in the vitreous, retina, or choroid of retinas from treated animals. Scale bar, 50 μm.

choroidal neovascularization both *in vitro* and *in vivo*. Previously, we have reported that specific HDAC inhibition has potential therapeutic value to be used as a novel target in developing angiogenic inhibitors.[14] HDAC inhibitor may suppress the VEGF gene in an indirect manner by down-regulating HIF-1α with increasing p53 and VHL under conditions of hypoxia.[14] Recently, HDAC inhibitor was also known to cause histone acetylation of VEGF promoter regions, which may directly induce suppression of VEGF gene expression.[28] Moreover, the angiogenesis-related gene modulation by HDAC inhibitors was reported.[29] The blood vessel growth in retinal and choroidal neovascularization correlates with the expression of VEGF and its receptors.[2] In this study, we showed that HNHA significantly inhibits VEGF-induced tube formation and cell migration of HUVECs (Figure 2). We already revealed that G_2/M phase cell cycle arrest, which is associated with the increase of $p21^{WAF1}$ expression, caused the antiproliferative activity of HNHA on HUVECs (Figure 1). We presented significant inhibitory effect of HNHA on retinal and choroidal neovascularization. HNHA reduced the incidence of clinically significant vascular leakage in OIR and an experimental model of laser-photocoagulation-induced CNV. It was consistent with histologic findings of significantly less number of neovascular vessels in HNHA-treated groups. That is, HNHA significantly reduced retinal neovascularization in OIR (Figure 3) as well as choroidal neovascularization in the animal model of laser-photocoagulation-induced CNV (Figure 4), which was as effective as SAHA. Moreover, 10 μM HNHA showed no effect on cell viability of HUVECs and no retinal toxicity. Based on these results, it is possible that HNHA may attenuate retinal neovascularization in OIR and laser-photocoagulation-induced CNV through a direct antiangiogenic effect without cytotoxic effect.

Given the well-documented *in vitro* antiangiogenic activity and *in vivo* antiangiogenic effect on retinal and choroidal neovascularization in this study, HNHA, a novel HDAC inhibitor, could be a new antiangiogenic agent to inhibit retinal and choroidal neovadcularization.

Materials and Methods

Materials. HNHA and SAHA were synthesized by our laboratory according to a patented procedure (Korean Patent 10-0620488). All stock solutions were prepared in DMSO and stored at −20 °C. EGM-2 was purchased from Lonza (Walkersville, MD). Dulbecco's modified Eagle medium,

antibiotics, and fetal bovine serum (FBS) were purchased from Life Technology (Grand Island, NY). PVDF membranes and the enhanced chemiluminescence (ECL) kit were purchased from Millipore (Bedford, MA) and Pierce (Rockford, IL), respectively. Rabbit antiacetylated histone polyclonal antibodies and mouse antitubulin monoclonal antibodies were obtained from Upstate Biotechnology (Lake Placid, NY). Mouse antiacetylated tubulin monoclonal antibodies were from Sigma-Aldrich (St. Louis, MO), and rabbit anti-$p21^{WAF1}$ polyclonal antibodies were from Santa Cruz Biotechnology (Santa Cruz, CA). HRP-conjugated sheep antimouse and donkey antirabbit antibodies were purchased from GE healthcare (Buckinghamshire, U.K.). The AK-500 kit was obtained from Biomol (Butler Pike, PA). Matrigel and Transwell plates were from Collaborative Biomedical Products (Bedford, MA) and Corning Costar (Cambridge, MA), respectively. C57BL/6 mice were purchased from Samtako (Korea). Care, use, and treatment of all animals in this study were in strict accordance with the ARVO statement for the Use of Animals in Ophthalmic and Vision Research.

***In Vitro* HDAC Assay.** Cultured cells were lysed with 0.5% Triton X-100 containing phosphate buffer (pH 8.0), and nuclear pellets were collected by centrifugation. HDAC activity was assayed from 10 μg of nuclear protein extract using a commercially available kit (AK-500). Assays were performed in a 96-well plate according to the manufacturer's instructions. Fluorescent, deacetylated substrate was measured with a FL600 Microplate Reader (Bio-Tek Instrument, Inc., Winooski, VT).

Cellular Proliferation and Viability Assays. HUVECs were maintained at 37 °C under a humidified, 5% CO_2 atmosphere in EGM-2 supplemented with 10% (v/v) heat-inactivated FBS. For measurement of cellular proliferation, cells were seeded in 96-well plates and 24 h later, treated with HNHA or SAHA for 24, 48, or 72 h. Stock solutions of HNHA and SAHA were prepared immediately before use. Proliferation was measured using the 3-(4,5-dimethylthiazol-2-yl)-2,5-diphenyltetrazolium bromide (MTT) assay. For measurement of cell viability, HUVECs were seeded in 24-well plates, and 24 h later, treated with HNHA or SAHA for 72 h. Cells were detached with trypsin-EDTA, and the cell suspension was incubated with an equal volume of 0.4% trypan blue reagent. Cells excluding the trypan blue dye (i.e., viable cells) were counted under the IX70 fluorescence microscope at 960× magnification.

Western Blot Analysis. HUVECs grown in 100 mm dishes were treated with HNHA or SAHA for 6 or 12 h. The cells were then washed and harvested by centrifugation. Protein extracts were separated by 12.5% SDS−PAGE and transferred to PVDF membranes. Membranes were blocked, incubated overnight at 4 °C with antibodies against acetylated histone, acetylated tubulin, or $p21^{WAF1}$, and then incubated with α-rabbit or α-mouse antibodies. Signals were detected using an ECL kit.

Cell Cycle Analysis. HUVECs were seeded in 60 mm dishes, grown for 24 h, and exposed to serum-restricted conditions (0.5% serum) for 16 h to induce synchronization. The cells were then treated with HNHA or SAHA for 24 h in the presence of 10% serum. Cells were harvested, fixed in 70% ethanol, resuspended in PBS (pH 7.4), and treated with RNase (80 μg/ml) and propidium iodide (50 μg/mL) for 1 h at 37 °C. DNA histograms were then obtained using a Beckton-Dickenson FACS Vantage flow cytometer system (Beckton-Dickenson, San Jose, CA). The cell cycle distribution was analyzed using Cell Quest software (Version 3.2, Beckton-Dickenson).

Tube Formation Assay. Tube formation was assayed as previous described.[30] HUVECs (1×10^5 cells) were seeded on the surface of the Matrigel and treated with 10 μM HNHA or VEGF for 18 h. Morphological changes were observed under a microscope and photographed at a 200× magnification. Tube formation was measured by counting the number of tube junctions among connected cells in randomly selected fields at a 100× magnification (Carl Zeiss, Chester, VA) and dividing this number by the total number of cells in the same field, and quantified as percentage (%) of nontreated control.

Endothelial Cell Migration Assay. Chemotactic motility of HUVECs was assayed as detailed elsewhere.[28] Migration assays were performed using a Transwell chamber system with 8.0 μm pore-sized polycarbonate filter inserts (Corning Costar, Cambridge, MA). Cells were seeded in the upper well of the chamber in the presence or absence of HNHA, while VEGF was placed in the lower wells. The cells migrating to the lower side of the filter were stained with hematoxylin and eosin, then counted at 100× magnification. Ten fields were counted per filter.

Oxygen-Induced Retinopathy. OIR was induced as detailed previously.[25,26] Briefly, newborn mice were randomly assigned to experimental ($n = 8-10$) and control ($n = 8 - 10$) groups. At P7, mice were subjected to hyperoxia (75% ± 0.5% O_2) for 5 days (to P12) and then returned to normoxic conditions (ambient air) for 6 days. At P14, a subset of animals received intravitreous injection of 10 μM/1 μL SAHA ($n = 8-10$) or HNHA ($n = 8-10$) in one eye and 1 μL of PBS in the remaining eye.

Laser Photocoagulation-Induced CNV. CNV was induced in 7−8 week-old female C57BL/6J mice by laser photocoagulation using a previously described method.[27] The pupils of anesthetized animals were dilated with 1% tropi-

(27) Kim, J. H. Antiangiogenic effect of deguelin on choroidal neovascularization. *J. Pharmacol. Exp. Ther.* **2008**, *324*, 643–647.

(28) Sasakawa, Y. Antitumor efficacy of FK228, a novel histone deacetylase inhibitor, depends on the effect on expression of angiogenesis factors. *Biochem. Pharmacol.* **2003**, *66*, 897–906.

(29) Deroanne, C. F. Histone deacetylases inhibitors as anti-angiogenic agents altering vascular endothelial growth factor signaling. *Oncogene* **2002**, *21*, 427–436.

(30) Min, J. K. Receptor activator of nuclear factor (NF)-kappaB ligand (RANKL) increases vascular permeability: impaired permeability and angiogenesis in eNOS-deficient mice. *Blood* **2007**, *109*, 1495–1502.

camide (Alcon Laboratories Inc., Forth Worth, TX). Three 831 nm laser diode beams (75 μm spot size, 0.1 s duration, 120 mW) were delivered to each 3, 6, 9, and 12 o'clock position of two separate sections of the optic disk by using an indirect head set delivery system (OcuLight; Iridex Corporation, Mountain View, CA) and a hand-held +78 diopter lens. All animals included in the study underwent successful rupture of Bruch's membrane, as indicated by bubble formation or an audible pop. A subset of animals were intravitreously injected with 10 μM/1 μL SAHA or HNHA 10 days after laser photocoagulation, when maximal CNV began. These experiments were repeated at least 25 times ($n = 25$ for each group).

Qualitative Assessment of Retinal and Choroidal Neovascularization. Mice subjected to OIR were deeply anesthetized and perfused through the tail vein with high molecular weight (MW = 50,000) fluorescein-conjugated dextran (dissolved in PBS Sigma-Aldrich) at P17. One hour later, the eyes were enucleated and fixed in 4% paraformaldehyde for 4 h. The retinas were dissected, flat-mounted in Dako mounting medium (DakoCytomation, Glostrup, Denmark), and viewed by fluorescence microscopy (BX50, OLYMPUS, Japan) at 4× magnification. Animals undergoing laser-photocoagulation were perfused with fluorescein-conjugated dextran 14 days after surgery, and the eyes were processed as described above. The eyecups were flat-mounted in Dako mounting medium (DakoCytomation, Glostrup, Denmark) and viewed by fluorescence microscopy at a 100× magnification. For both models, at least six animals were examined per treatment group.

Quantitative Assessment of Retinal and Choroidal Neovascularization. At P17, the eyes were removed from animals with OIR, fixed in 4% paraformaldehyde in 0.1 M phosphate buffer for 24 h, and embedded in paraffin. The cornea was sectioned parallel to the optic nerve to obtain 5 μm thick, sagittal slices that were 30 μm apart. The sections were stained with hematoxylin and eosin to assess retinal vasculature via light microscopy (Zeiss). Vascular lumens on the vitreal side of the inner limiting membrane were counted in at least 10 sections from each eye (at least five on each side of the optic nerve) by two independent observers blinded to treatment. The average number of intravitreal vessels per section was calculated for each group. At least six animals were included in each treatment group.

In animals with CNV, eyes were collected at 14 days after laser photocoagulation and were processed as described above. The center of laser-photocoagulation site was sectioned, at 10 μm intervals, into 4−5 μm thick sagittal slices. Vessels in the subretinal fibrovascular membrane were counted in hematoxylin and eosin-stained sections. Counts were obtained for five sections per laser-photocoagulation site by two independent, blinded observers. In each treatment group, over 100 sites were examined from at least 25 animals.

TUNEL Assay. SAHA or HNHA was intravitreously injected to 7- to 8-week-old female C57BL/6J mice. For negative control, 1 λ PBS was injected. The mice were sacrificed at 3 days after 10 μM/1 μL SAHA or HNHA injection, and enucleated. Enucleated globes were fixed in 4% paraformaldehyde in 0.1 M phosphate buffer for 24 h, and embedded in paraffin. TUNEL staining was performed with a kit (ApopTag Fluorescein Green; Intergen, Purchase, NY), according to the manufacturer's instructions. TUNEL-positive cells were evaluated in randomly selected fields at a 400× magnification viewed under fluorescein microscopy (BX50, OLYMPUS, Japan).

Statistical Analysis. Differences between groups were evaluated using Student's unpaired t test (two-tailed). All data are expressed as mean ± SD. $P \leq 0.05$ was considered significant.

Abbreviations Used

AMD, age-related macular degeneration; CNV, choroidal neovascularization; EGM-2, endothelial cell medium-2; HDAC, histone deacetylase; HNHA, *N*-hydroxy-7-(2-naphthylthio) heptanomide; HUVECs, human umbilical vein endothelial cells; MTT, 3-(4,5-dimethylthiazol-2-yl)-2,5-diphenyltetrazolium bromide; OIR, oxygen-induced retinopathy; ROP, retinopathy of prematurity; SAHA, suberoylanilide hydroxamic acid.

Acknowledgment. This study was supported by grants from the National R&D Program for Cancer Control, Ministry of Health & Welfare (0620360-1), the Basic Research Program of the Korea Science & Engineering Foundation (R01-2004-000-10212-0), the Bio-Signal Analysis Technology Innovation Program (M1064501001-06n4501-00110) of the Ministry of Science and Technology (MOST), the Korea Science and Engineering Foundation (KOSEF) and the Brain Korea 21 Project, Republic of Korea.

MP800178B